ELSEVIER

Journal of Power Sources 74 (1998) 219–227

JOURNAL OF POWER SOURCES

A consideration of the morphology of electrochemically deposited lithium in an organic electrolyte

Jun-ichi Yamaki [a], Shin-ichi Tobishima [b,*], Katsuya Hayashi [b], Keiichi Saito [b], Yasue Nemoto [b], Masayasu Arakawa [b]

[a] *Institute of Advanced Material Study, Kyushu University Kasuga Koen 6-1, Kasuga-shi, Fukuoka-ken, 816-8580, Japan*

[b] *Nippon Telegraph and Telephone Corporation, NTT Integrated Information and Energy systems Laboratories, Tokai-Mura, Ibaraki-ken, 319-1193, Japan*

Received 16 October 1997; accepted 24 February 1998

Abstract

Lithium rechargeable cells with lithium metal anodes are widely considered to have the highest energy density among comparable cells. However the life cycle and thermal stability of these cells must be improved. The poor performance of lithium metal cells is mainly explained by lithium dendrite growth. With a view to overcoming this problem, we considered the lithium deposition mechanism. We have been carrying out various experiments on the lithium deposition behavior. In this paper we used these results to propose the current and most likely lithium deposition mechanism. We suggest that lithium dendrites may be called whiskers because their shape satisfies the definition of whiskers as 'fibrous crystals'. Their tip morphology remains unchanged during their growth, which means they grow from the base in the same way as whiskers of tin from thin films under stress. Lithium deposited under a protective film will experience stress because the deposition is non-uniform. The protective film will break in order to release this stress thus, lithium whiskers may then grow in the form of extrusions. To support our assumption, we calculated the possible morphology of the lithium with the boundary condition that pressure induced by the surface tension is the same throughout the lithium surface. The calculation indicated three types of shape depending on the value of the surface tension and internal pressure. If lithium deformation is limited by the creep strength of bulk lithium and the lithium whiskers, the whisker growth is described by the calculated shape.

Keywords: Lithium; Electrolyte; Dendrite; Deposition

1. Introduction

Rechargeable cells with lithium metal anodes have a very high energy density. However the life cycle and thermal stability of these cells must be improved. We made AA size lithium metal anode cells with amorphous V_2O_5 cathodes. The energy of these cells is 2 Wh, have a life cycle of 150 cycles [1] and are thermally safe up to 130°C. However, at a low discharge rate cycle, their life cycle is 50 cycles and the thermal stability falls to 125°C. The poor performance of the lithium metal cells is mainly explained by lithium dendrite growth.

We have been carrying out experiments on the lithium deposition behavior for about 10 years in view of analyzing cell performance and safety in relation to the lithium deposition mechanism [2–6]. Some examples are outlined below. We have made scanning electron microscope (SEM) observations of lithium deposition and investigated the relationship between morphology and experimental conditions by using coin type cells with sandwich structure electrodes and AA size cells with jelly roll electrodes. The experimental factors we investigated consisted of the dependence of morphology on the charge and/or discharge current density, the charge and/or discharge capacity, the environmental temperature, the electrolyte materials including solvent and solute, the electrolyte additives, the methods of lithium anode construction and the influence of the electrode stack pressure [2,3,5,6]. We also used the video recording for the in situ observation of lithium growth [3,5]. We were the first to measure the specific surface area of a lithium anode spirally wound in an AA-size cell and proved quantitatively that the surface area increases with a decrease in the discharge current and

* Corresponding author.

0378-7753/98/$19.00

an increase in the number of charge–discharge cycles [4]. In addition, we have undertaken many cell safety tests including thermal abuse tests such as a heating test; electrical abuse tests such as external short, overcharge and forced discharge tests; and mechanical abuse tests such as nail penetration and crush tests with a round bar and a flat plate [1,4,5]. These experiments have provided us with many and various data for analysis in relation to lithium deposition morphology. In addition, a large amount of work has produced experimental data on lithium deposition behavior. However, the current theoretical approach to the lithium deposition mechanism is insufficient. In this report, we would like to propose the lithium deposition mechanism which we consider to be the most likely approach based on our various experimental results mentioned above.

When a cell is charged, lithium is deposited on the lithium substrate of the anode. The plated lithium is not flat but fiber-like. When the cell is discharged, the lithium anode is dissolved, and sometimes the fiber-like lithium is cut and isolated from the anode substrate [2]. This isolated lithium, known as 'dead lithium,' is electrochemically inactive but chemically active. During cycling, the dead lithium accumulates on the anode. This means that anode active material is consumed during cycling. As a result, the cell life cycle becomes shorter at a low rate discharge. The dead lithium also reduces thermal stability [3]. The increase in the surface area of the anode is greater after a low rate discharge than after a high rate discharge, which means that the amount of dead lithium is larger after a low rate discharge [4]. For example, it has been found that the lithium surface area after only six low discharge cycles is twice that with high-discharge cycles [4]. When the cell temperature increases for any reason, the reaction between the lithium and the electrolyte is accelerated and generates heat [5]. Sometimes, the amount of heat is large enough to result in thermal run-away. Stack pressure perpendicular to each electrode suppresses the creation of dead lithium [6], and improves the thermal stability. However, the cell is unsafe if the stack pressure at any part of an electrode is insufficient due to a manufacturing defect. Therefore, we need to make fundamental improvements to the lithium electrode.

If the lithium plating morphology is flat and fiber-like lithium is not formed, the lithium metal cell has a longer life cycle and better thermal stability. There have been many studies aimed at reducing the creation of fiber-like lithium by the use of additives in electrolytes. Besenhard et al. [7] found that the deposited lithium was particle-shaped when *cis*- or *trans*-decalin was added to $LiClO_4$/propylene carbonate (PC) electrolyte. Though there was no change in the cycling efficiency, the long-term storage characteristics improved. Recently, Kanamura et al. [8] also reported particle-shaped deposition resulting from the addition of HF to $LiClO_4$/PC electrolyte. Osaka et al. [9] undertook a precise study of the effect of H_2O and CO_2 in $LiClO_4$/PC, and found that CO_2 is effective protection against H_2O. They reported these additive effects are caused by the modification of the protective films. In this situation, it is interesting to study the mechanism by which fiber-like lithium is created. We believe that it may be possible to link the mechanism to the effect of the additives.

2. Morphology of deposited lithium

There have been many reports on the morphology of the lithium that is electrochemically deposited in various kinds of organic electrolyte [6,8,10–15].

Koshina et al. [16] reported that there are three kinds of morphology; dendritic, granular and mossy. The dendritic lithium from their definition is so-called fiber-like lithium. They used $LiPF_6$/PC–ethylene carbonate (EC) electrolyte and found that mossy lithium is formed when the deposition current is small and the salt concentration is high. The mossy lithium provided a high cycling efficiency.

Matsui and Takeyama [17,18] studied the morphology of the electro-deposition and dissolution process by the Monte Carlo technique under a two dimensional lattice scheme on the basis of deposition at the surface of the deposited product and no mass transfer of lithium in the lithium electrode. The shape is rod-like with a branch under the conditions corresponding to high current deposition. This is because the deposition occurs at the tip of the deposited product. When the electrode particle charge and the sticking probability are small (corresponding to low current deposition), the shape is leaf-like or flat because of activated ion diffusion on the electrode surface. If only a small part of the electrode is active, the deposition is shaped like a temple bell. During stripping, rod-like (with branch) deposition products are separated from the electrode, and much of the deposition product can not be stripped. Deposition products which are flat or temple bell-shaped can be stripped without isolation.

The lithium morphology at the beginning of the deposition was measured by Morigaki et al. [19] using in situ atomic force microscopy (AFM). There were grains with a size of 1–2 μm, and in the grain were thin lines of 100–300 nm and flat parts on native lithium surface. The flat region was composed of small elliptical particles of about 60 nm in size. When lithium was deposited for 0.6 C cm^{-2}, small particles 200–1000 nm in size were deposited on the thin lines and grain boundaries in $LiClO_4$/PC. Lump-like growth was observed in $LiAsF_6$/PC along the line [19].

An electrochemical quartz crystal microbalance (EQCM or QCM) can be used to estimate the surface roughness of deposited lithium. Mori et al. [20] reported that a $LiPF_6$/PC electrolyte displayed the highest cycling efficiency and the resistance parameter from QCM did not increase upon

deposition, whereas the resistance parameter for $LiClO_4$/PC did increase because of the surface roughness.

The authors have observed lithium deposition on a stainless steel (SS) substrate in 2MeTHF–EC/$LiAsF_6$ electrolyte at a deposition current of 0.5 mA/cm^2 [2,3]. A SEM was used for the observation. After 1 min, small particles about 0.1 μm in diameter were deposited. Fiber-like lithium was also deposited which had a diameter of about 0.1 μm and was 1 μm long. After 3 min of deposition, no particle-like lithium could be observed and only the fiber-like lithium was present, some of which had a thicker diameter of 0.5 μm. The particle-like lithium was growing and becoming fiber-like. When the deposition was continued for 10 min, particle-like or amorphous lithium (diameter: about 1 μm) was deposited among the fiber-like lithium (Some were 1 μm in diameter). When the deposition current was changed, the fiber-like lithium showed a tendency to become thinner with increasing current. When the deposition current was small (less than 1.5 mA/cm^2), a lot of amorphous or particle-like lithium was observed. The temperature dependence was also examined and it was found that the diameter of the deposited lithium was very small (about 0.3 μm) at -10°C, even after 5 min of deposition at 0.5 mA/cm^2.

Electrode stack pressure also changes the lithium morphology [6] [21,22]. In a practical cell, stack pressure is usually applied to the lithium anode. This makes it interesting to study the effects of pressure on lithium morphology. As lithium is a soft metal, fiber-like lithium deforms and achieves a flat surface. Surface observation reveals that lithium deposited under pressure is metallic silver while that deposited without pressure is gray or dark brown.

As a typical example, Fig. 1 shows the morphology of the lithium deposited in ethylene carbonate/2-methyltetrahydrofuran/$LiAsF_6$ at 0.5 mA/cm^2 for 10 min on a stainless steel substrate. The shape is a rod with kinks. The fiber-like lithium can be called a whisker because 'a whisker' is defined as 'a fibrous crystal' without any definition of its growth mechanism [23]. As the growth of potassium whiskers has been reported [24], lithium an alkaline metal, may also grow whiskers. The many studies of whiskers that have been undertaken [25] have shown that there are two kinds of growth mechanism. Early proposals called for growth from the tip, and later, growth from the base was discovered. The possibility of growth from the base because the Monte Carlo method calculated by Matsui and Takeyama [17,18] based on growth from the tip cannot simulate the deposition of rod-like lithium without branches.

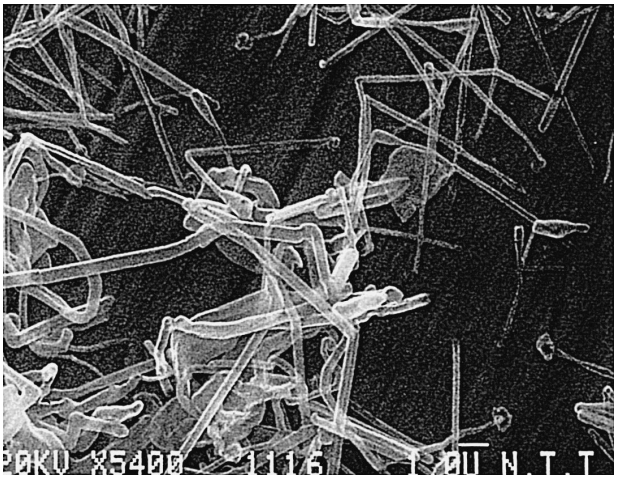

Fig. 1. SEM photograph of lithium deposited in EC/2MeTHF//$LiAsF_6$ electrolyte at 0.5 mA/cm^2 for 10 min.

It is reported that tin whiskers grow from the base and not from the tip. Franks [26] reported that, ''The tests described in this section indicate that the restriction to soft metals is merely due to the ease with which the free extrusion limit may be reached while still being inhibited by neighboring stronger material. In principle, it should be possible to produce whiskers on any metal if the extrusion conditions are satisfied.'' Tu [27] also studied whisker growth in bimetallic Cu–Sn thin film and reported that the compression stress on Sn film is caused by the formation of Cu_6Sn_5 at the interface. He also reported that if the Sn surface is free of oxide, it becomes an effective source and sink for vacancies. However, if the Sn surface forms an oxide, the surface loses this characteristic. In this case, vacancy sources become incapable of maintaining a normal gradient of vacancies. The film will then experience stress and the Sn surface will break to release it. Whiskers then grow on the surface. As lithium is a soft metal and the surface is covered with protective film [28] made of Li_2O, LiF, Li_2CO_3, LiOH, etc., lithium whiskers should grow namely from the base with the same mechanism as tin. The difference is that the tin whiskers are created by stress in the tin substrate while lithium whiskers are formed by electrochemical deposition. We believe that lithium deposited on a lithium substrate, causes stress in the lithium substrate. We will discuss the experimental evidence more precisely later in this paper.

3. Mechanism of electrochemical creation of lithium whiskers

We propose the following mechanism for lithium whisker creation by electrochemical deposition based mainly on observations of lithium morphology in EC/2MeTHF//$LiAsF_6$ electrolyte [2,3]. Fig. 2 shows a schematic representation of the mechanism.

(1) A working electrode of lithium foil and a counter electrode are placed in an organic electrolyte. The surface of the lithium electrode is covered with protective film.

(2) With an external power supply, the lithium electrode potential is set to a negative value (just below the Li/Li^+ potential). Lithium ions in the electrolyte move to the lithium surface through the protective film.

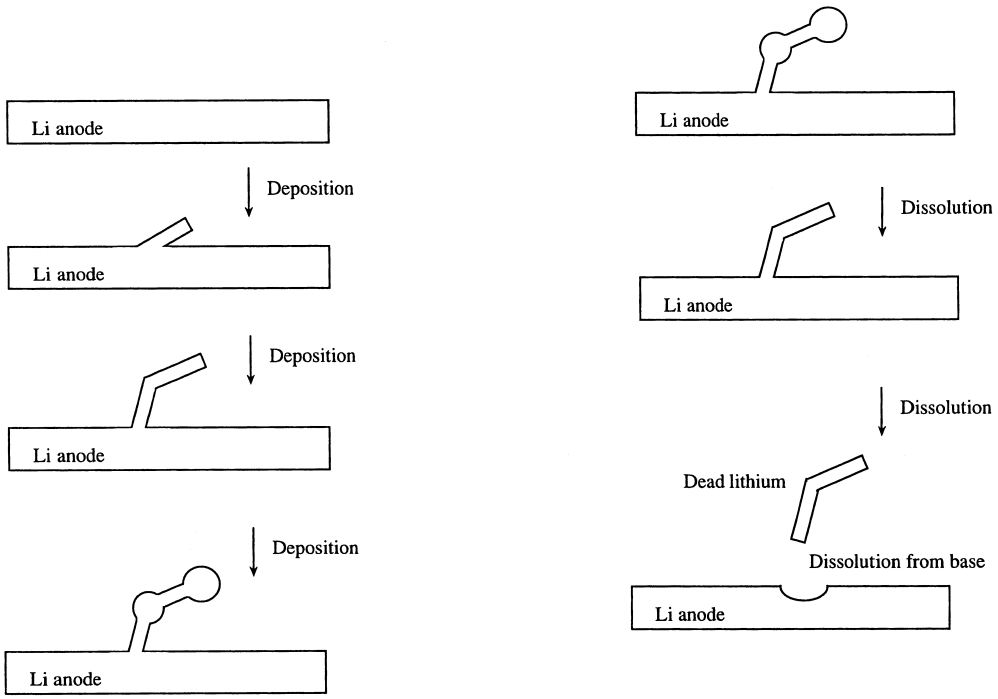

Fig. 2. Our model of lithium deposition and dissolution.

(3) Lithium is deposited on the lithium anode under the protective film without seriously damaging the film.

(4) The deposition points are the points where the protective film has a higher lithium ion conductivity. Crystalline defects and grain boundaries in the lithium also initiate deposition [19].

(5) As lithium is not deposited uniformly for the reason mentioned above, mechanical stress is created in the lithium electrode under the protective film.

(6) The stress causes the transport of lithium atoms, probably through the grain boundaries. This means the lithium deforms to relieve the stress. The lithium is not transported freely but is limited by a force created by the lithium surface tension (including the effect of the protective film) at curved surfaces, crystalline defects and grain boundaries.

(7) The protective film is broken by the stress at certain points on the lithium surface. The lithium is extruded through the resulting holes and grows in the form of whiskers.

(8) After a lithium whisker has grown, lithium continues to be deposited on the lithium substrate but not on the tips of the whisker. After a long period of deposition, the electrode is covered with long whiskers. This hinders lithium ion transport in the electrolyte to the electrode surface. Then, lithium begins to be deposited on the tip and kink points of the whiskers, where there are crystalline defects. The morphology of the deposited lithium is particle-like or amorphous. As there are many kink points, the current density of the lithium deposition becomes very low. This low current density may create particle-like or amorphous lithium, rather than whiskers. Thus, the morphology of the lithium as a whole becomes mushroom-like [2].

The dissolution of plated lithium may follow the reverse of the plating process. First, the particle-like lithium on the tips and kink points is dissolved. Next, the whiskers are dissolved at the base. If the dissolution current is larger than the deposition current, the dissolution is not completely the reverse of the deposition. In this case, a larger amount of lithium dissolves from the tips and kink points. This situation is determined by the ease of lithium ion transport from the base lithium. When the dissolution current is smaller than the deposition current, a smaller amount of lithium dissolves from the tips and kink points. During this process, the whiskers are sometimes cut from the lithium substrate and become dead lithium.

When the diameter of the whisker is small as a result of formation at a high deposition rate and/or at a low deposition temperature, the amount of dead lithium is large because the whisker is easily cut.

4. Experimental evidence for the mechanism

We believe that our deposition mechanism is acceptable for the following reasons discussed below.

(1) Lithium deposition was observed with an optical microscope in a dry room (relative humidity less than 2% [29]). Fig. 3 shows photographs of whiskers. The electrolyte is PC/$LiClO_4$. A tip is visible slightly to the right of the center in Fig. 3a. As shown in Fig. 3b, after 10 s of

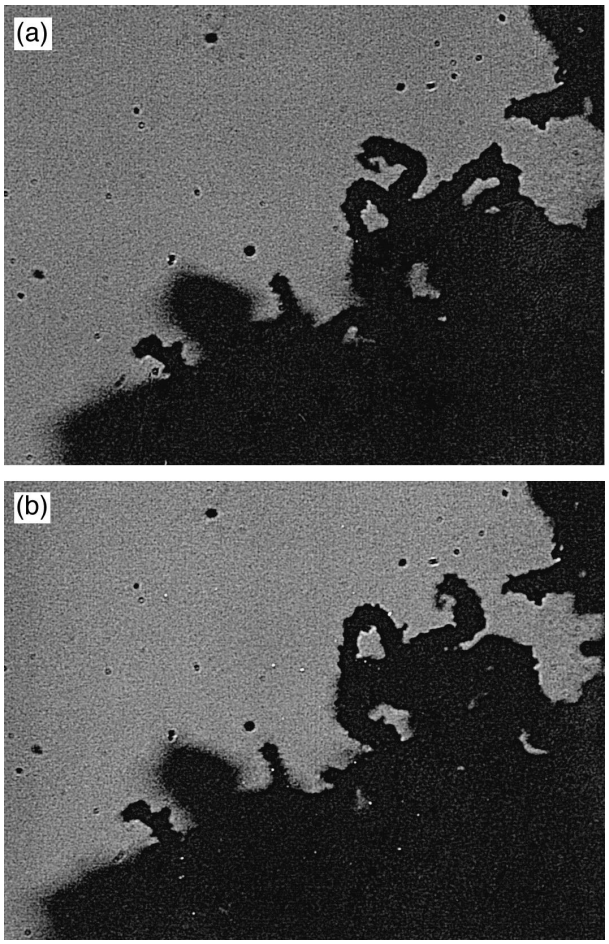

Fig. 3. In situ observation of lithium deposition in PC//$LiClO_4$. (a) morphology of deposited lithium (b) morphology of deposited lithium 10 s later.

deposition, the tip moved to the right as a result of growth from the base without any change in the tip shape. However, the growth mechanism is still unclear, because we cannot observe the base of the whisker directly.

(2) The lithium whiskers begin to grow after some induction time then they stop growing suddenly. The whisker growth region on the lithium electrode moves from time to time. These phenomena are in good agreement with that of a proper whisker induced by stress.

(3) Kinks also observed in the whisker as with a proper whisker.

(4) The diameter of the whisker seems to remain the same during growth. This evidence supports the suggestion of lithium extrusion through a hole in the protective film.

(5) Particle-like or amorphous lithium depositions were observed experimentally at kinks [3].

(6) There is a tendency for a higher discharge current to improve the life cycle on the basis of an experimental result on our AA-size cell [1]. This corresponds to the theory that when the dissolution current is large, a larger amount of lithium dissolves from the tip and kink points resulting in the creation of less dead lithium.

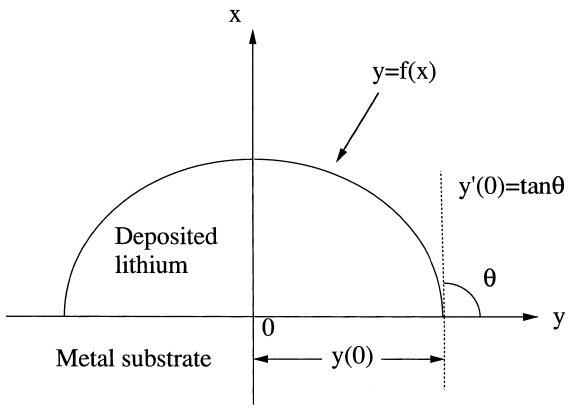

Fig. 4. Coordinates of lithium surface.

(7) It is usually accepted that the protective film is not broken by the lithium deposition from the SEI model proposed by Peled [30].

5. Some considerations related to lithium surface tension

Proper whiskers grow from arrays of dislocation loops which form spirals or helices. It is important to discuss the dislocation mechanism to understand the whisker growth mechanism. However, this mechanism is not easy to consider because it may vary for different materials. There is another approach for dendritic structures which focuses on surface tension. These structures are observed at the interface of two immiscible fluids with different viscosities, confined between two parallel closely positioned plates, when pressure is applied to the less viscous fluid [31]. The structure varies depending on the amount of applied pres-

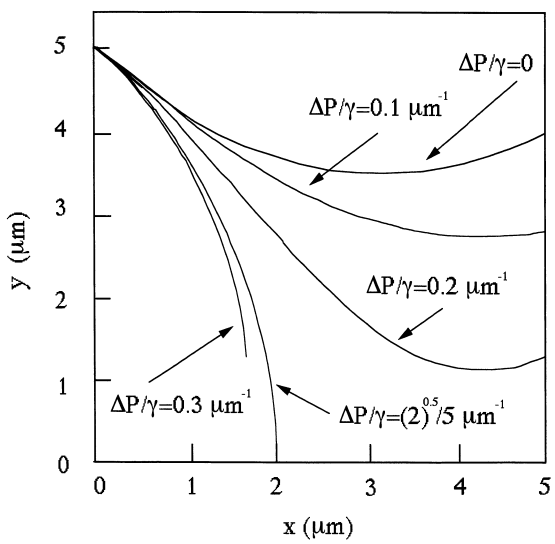

Fig. 5. Surface shape of deposited lithium calculated from Eq. (4). [Initial condition: $y(0) = 5\ \mu m,\ y'(0) = -1$].

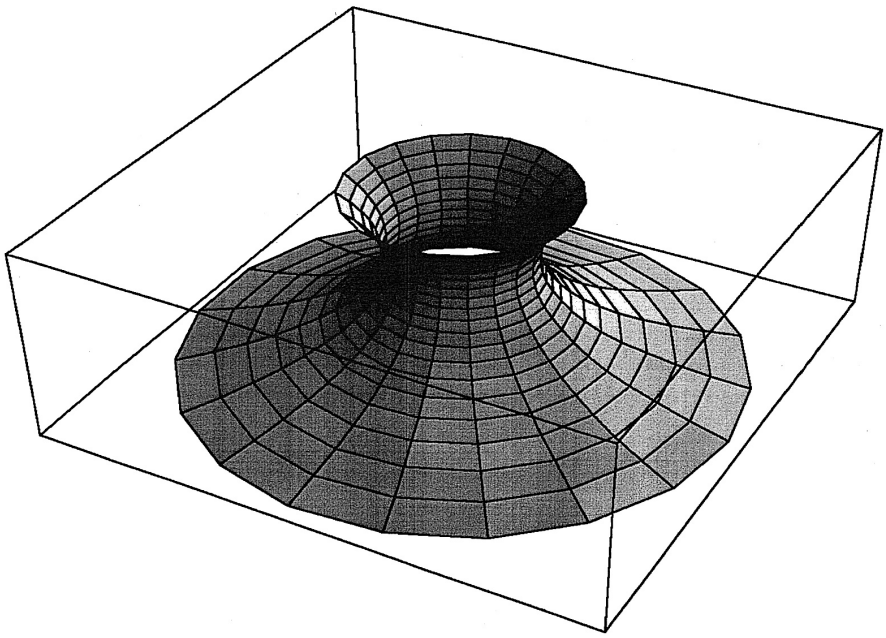

Fig. 6. Three dimensional image of the solution of Eq. (4) with the condition $\Delta P/\gamma = 0$.

sure. A fluid dynamics mathematical model describes the interfacial dynamics of pressure at a boundary induced by the surface tension of two fluids.

As lithium is a soft metal and deforms easily, we tried to examine the effect of surface tension. We calculated a possible morphology for the lithium under the boundary condition that the pressure induced by surface tension is the same throughout the lithium surface. If the lithium is deposited on a flat lithium substrate, the pressure must be zero, because it is the same throughout the lithium surface. The calculation is therefore only useful for deposition on a different solid metal. Although it is an estimation of the steady state after deposition, it will have some meaning as a first step in studying lithium morphology.

If we suppose that lithium is deformed as a result of a pressure difference on the lithium surface (ΔP) caused by the surface tension, the following equation applies:

$$\Delta P = \gamma(1/R_1 + 1/R_2) \tag{1}$$

where γ is the surface tension on a lithium surface (or surface energy), and R_1 and R_2 are principal radii of curvature of the surface. If the lithium surface is symmetric around the x-axis (Fig. 4), we can describe the lithium surface by the distance between the surface and the x-axis; $y = f(x)$. In this case, R_1 and R_2 are expressed as follows [32];

$$R_1 = -\frac{\left[1 + (\mathrm{d}y/\mathrm{d}x)^2\right]^{3/2}}{\mathrm{d}^2y/\mathrm{d}x^2} \tag{2}$$

$$R_2 = y\left[1 + (\mathrm{d}y/\mathrm{d}x)^2\right]^{1/2} \tag{3}$$

From Eqs. (1)–(3), we have

$$\mathrm{d}^2y/\mathrm{d}x^2 = \frac{-\Delta P/\gamma\left[1 + (\mathrm{d}y/\mathrm{d}x)^2\right]^{3/2} + \left[1 + (\mathrm{d}y/\mathrm{d}x)^2\right]}{y} \tag{4}$$

Eq. (4) shows that if the parameter $\Delta P/\gamma$ increases by a factor of n, the lithium surface shape is similar but with a radius of curvature smaller by a factor of $1/n$.

The dimension of $\Delta P/\gamma$ is $[\mathrm{L}]^{-1}$. If we use μm for x and y, the dimension of $\Delta P/\gamma$ is $\mu\mathrm{m}^{-1}$. We will use $\Delta P/\gamma$ as a parameter, because any value can be used for ΔP. We need two initial conditions to solve Eq. (4). We used the contact angle of the deposited lithium to the substrate [$y'(0)$], and the position where the lithium surface comes into contact with the substrate [$y(0)$] as shown in Fig. 4. Gravity was assumed to be negligible (See Appendix A).

A numerical calculation was undertaken from Eq. (4) using a personal computer PowerBook Duo 230 (Macintosh) and the Mathematica calculation program (NDSolve by Wolfram Research). The initial condition was $y(0) = 5$ μm and $y'(0) = -1$. We have three different kinds of solution depending on the $\Delta P/\gamma$ value. The results are shown in Fig. 5.

(i) $\Delta P/\gamma = (2)^{1/2}/5\ \mu\mathrm{m}^{-1}$ (general value is $2/y(0)[1 + y'(0)^2]^{1/2}$). The surface is a part of a sphere with a radius of $5(2)^{1/2}$ μm. We can easily expect the surface to be a sphere with a radius of $2\gamma/\Delta P$ from Eq. (1).

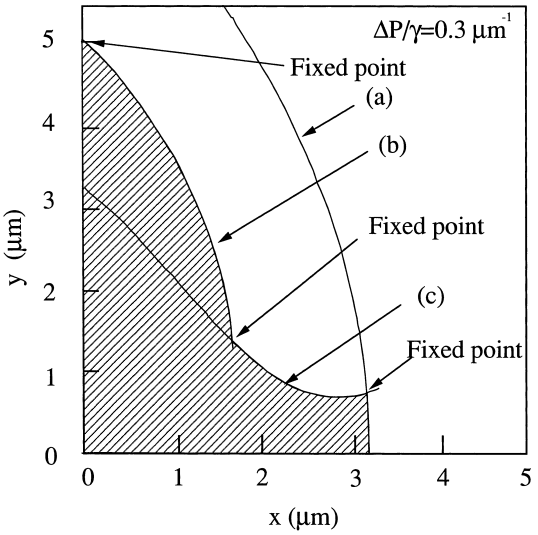

Fig. 7. Example solution for Eq. (4) obtained by a combination of the solutions shown in Fig. 5. All the curves satisfy the condition $\Delta P/\gamma = 0.3$ μm^{-1}. Curve (a) is a circle with a radius of $(2/0.3)$ μm. Curve (b) is that shown in Fig. 4. Curve (c) is similar to $\Delta P/\gamma = 0.2$ μm^{-1} in Fig. 4 but with a radius of curvature smaller by a factor of $2/3$. Lithium is in the hatched area.

(ii) $\Delta P/\gamma > (2)^{1/2}/5\ \mu m^{-1}$. The solution of $\Delta P/\gamma = 0.3\ \mu m^{-1}$ is shown in Fig. 5. The surface does not have solution near $y = 0$.

(iii) $\Delta P/\gamma < (2)^{1/2}/5\ \mu m^{-1}$

Two solutions for $\Delta P/\gamma = 0.1\ \mu m^{-1}$ and $\Delta P/\gamma = 0.2\ \mu m^{-1}$ are shown in Fig. 5. Here too, the surface has no solution near $y = 0$. There is a numerical solution for $\Delta P/\gamma = 0$; $y = A\cosh[(x + B)/A]$, where A and B are constants [33]. A three dimensional image of $y = \cos x$ $(-2 < x < 1)$ is shown in Fig. 6. The image was calculated using ParametricPlot3D of Mathematica (Wolfram Research).

We can make various shapes by combining three solutions within the condition $\Delta P/\gamma =$ constant as shown in Fig. 7. As mentioned above, if the parameter $\Delta P/\gamma$ increases by a factor of n, the lithium surface shape is similar but with a radius of curvature smaller by a factor of $1/n$. This means we can change the $\Delta P/\gamma$ value easily. However, we have to fix the point (or line) to a position as indicated in Fig. 7. If the point is free, the shape changes to a sphere.

6. Introduction of the fixed point

It is reported that the creep strength of bulk lithium is 60 psi $(4.1 \times 10^5\ Nm^{-2})$ for 2.2 h and the tensile strength of lithium is 84 psi $(5.8 \times 10^5\ Nm^{-2})$ at room temperature [34]. ΔP must be larger than $4.1 \times 10^5\ Nm^{-2}$ to make a mass transfer of lithium. Therefore, if ΔP becomes smaller than $4.1 \times 10^5\ Nm^{-2}$ at some area, the lithium does not deform. That area acts as a fixed point.

In general, a highly crystallized material has a higher creep strength than the non-crystallized stage of the same material. Therefore, a lithium whisker has a higher creep strength than bulk lithium. Let σ_c be the creep strength of the whisker $(\sigma_c > 4.1 \times 10^5\ Nm^{-2})$.

When the lithium is extruded through holes in the protective film, the surface tension may act to maintain the

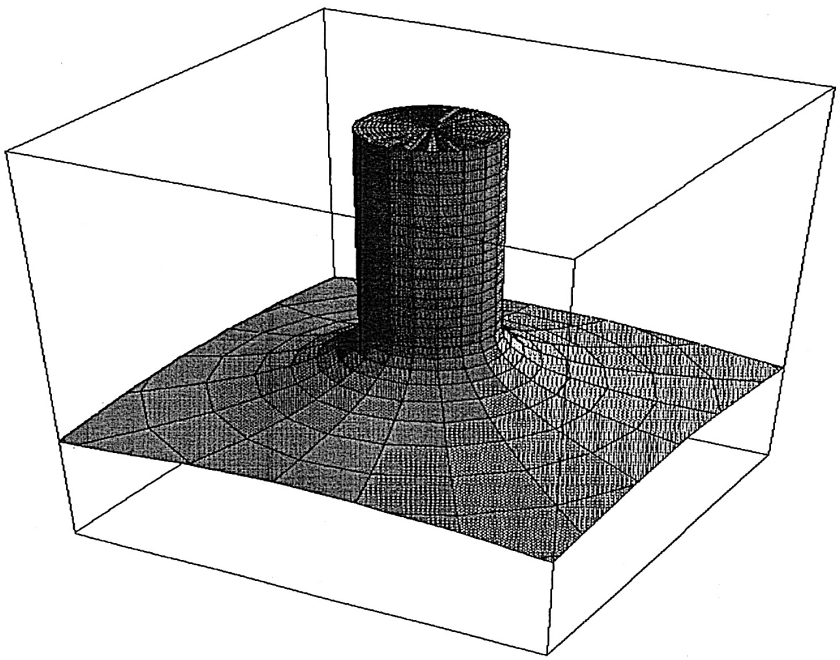

Fig. 8. Three dimensional figure of the whisker growth expected from our discussion.

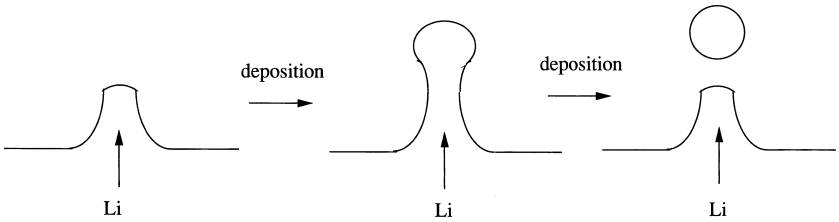

Fig. 9. A possible lithium deposition mechanism when the surface tension is large enough to deform the whisker.

hole size. In other words, the protective film seems not to be strong enough to deform the lithium because the film is thin and made of Li_2O, Li_2CO_3, LiOH etc. If the diameter of the lithium whiskers is about 2 μm, the surface shape near the hole may be the shape for $\Delta P/\gamma = 0.2\ \mu m^{-1}$ shown in Fig. 5 and the lithium may be extruded along the x-axis towards the right side of the figure. The lithium moves through the bottle-neck near $x = 4$ and after passing through the point, it may maintain its rod-like shape because of its high crystallinity. A three dimensional figure of the expected whisker growth is shown in Fig. 8. The bottle-neck will not expand because of ΔP which is caused by the surface tension. ΔP must be larger than $4.1 \times 10^5\ Nm^{-2}$ and smaller than σ_c. Therefore, $\gamma > 2.05\ Nm^{-1}$. There is no data available on lithium surface tension at room temperature, however it may be around 0.2 Nm^{-1}, because the surface tension of lithium is 0.22 Nm^{-1} (220 dyn/cm) at 1000°C ($\gamma = 425.2–0.16$ T, T: temperature K for 922–1307°C, γ:dyn/cm) [35]. It is probably possible to increase the surface tension to higher than 0.2 Nm^{-1} through the effect of the protective film. The surface tension can be an apparent surface tension including the effect of the protective film (surface tension of the protective film) and change in volume during the reaction to create the film.

In order to maintain the shape of the whisker, σ_c must be larger than the pressure caused by the surface tension. Therefore, the following relation has to be satisfied; $\sigma_c > \Delta P = \gamma/R$($R$:whisker radius). To date, we have not seen a lithium whisker with a diameter smaller than about 0.3 μm. If 0.3 μm is the critical radius, we have the following equation. $\sigma_c = 3.3 \times 10^6 \gamma\ Nm^{-2} > 6.8 \times 10^6\ Nm^{-2}$ If the surface tension is larger than σ_c, the whisker created by the extrusion is not stable. A model for such a deposition is shown in Fig. 9. At first, the lithium surface may be deformed by local non-uniform stress in the lithium. The surface shape may approximately follow the solution of $\Delta P/\gamma < (2)^{1/2}/5\ \mu m^{-1}$ (whose general value is $2/\{y(0)[1 + y'(0)^2]^{1/2}\}\ \mu m^{-1}$). Such a deformation cannot be avoided by modifying the surface tension to make it very high, because $\Delta P/\gamma = 0$ (this means $\Delta P = 0$) is one of the solutions. From this consideration, we think that a very high surface tension may not result in flat deposition but particle-like deposition.

Basically, we should limit our discussion to the shape after deposition. The internal pressure is different when lithium is moving because the pressure difference is the force required to move the lithium. Therefore, for example, the shape in Fig. 8 may be correct if the internal pressure is equalized at any location by annealing after the deposition.

7. Conclusion

From studies on tin whisker growth and the in situ observation of lithium dendrite growth, we found that lithium dendrites are whiskers and they may grow from their base during electrochemical deposition. We proposed a lithium deposition mechanism in which whisker growth occurs from the base. The deposited lithium may break the protective film and lithium whiskers may grow as extrusions through the resulting holes. To discuss our model precisely, we calculated the possible lithium morphology with the boundary condition that the pressure induced by surface tension is the same throughout the lithium surface. The shape corresponds to a steady state after deposition. Our calculation provided three types of shape depending on the value of the surface tension and the internal pressure. If we suppose that the pressure caused by surface tension must be larger than the creep strength, the solution is useful for explaining lithium deposition.

The following is currently the most possible conclusion while part of the conclusion is difficult to prove experimentally. ‘On the basis of our model, we believe that lithium is deposited as particles when the surface tension is large enough to deform lithium whiskers’. We expect this work to stimulate discussion on the theoretical approach to describing the lithium deposition mechanism and through the various discussions, our simulation method will be improved after scientifically necessary changes have been completed.

Acknowledgements

The authors wish to express their gratitude to Dr. I. Yamada for helpful discussions during the course of this research.

Appendix A. Gravity-neglecting approximation

If we wish to calculate the shape to a maximum height of z m, the change in pressure difference ΔP caused by gravity is less than $\rho\ gz$ where ρ is lithium density (5.34×10^2 kg m^{-3}) and g is gravity acceleration (9.8 m s^{-2}). As regards the solutions shown in Fig. 5, $\Delta P/\gamma$ is larger than 0.1 μm^{-1}. There is no data on lithium surface tension (γ) at room temperature. So, we assume γ is larger than 0.1 Nm^{-1}.Then, $\rho\ gz = 5.23 \times 10^3 z$ Nm^{-2}, $\Delta P > 0.1 \times 10^6 \gamma$ $Nm^{-2} > 10^4$ Nm^{-2}.Because $\rho\ gz$ must be negligible compared with ΔP, this approximation is useful for $z =$ about 10^{-2} m (10 000 μm). This z value is sufficient for the actual calculation.

References

[1] Y. Sakurai, S. Sugihara, M. Shibata, J. Yamaki, NTT Rev. 7 (1995) 60.
[2] I. Yoshimatsu, T. Hirai, J. Yamaki, J. Electrochem. Soc. 135 (1988) 2422.
[3] M. Arakawa, S. Tobishima, Y. Nemoto, M. Ichimura, J. Yamaki, J. Power Sources 43–44 (1993) 27.
[4] K. Saito, M. Arakawa, S. Tobishima, J. Yamaki, Denki Kagaku 62 (1994) 888.
[5] M. Arakawa, Y. Nemoto, S. Tobishima, M. Ichimura, J. Yamaki, J. Power Sources 43–44 (1993) 517.
[6] T. Hirai, I. Yoshimatsu, J. Yamaki, J. Electrochem. Soc. 141 (1994) 611.
[7] J.O. Besenhard, J. Guertler, P. Komenda, J. Power Sources 20 (1987) 253.
[8] K. Kanamura, S. Shiraishi, Z. Takehara, J. Electrochem. Soc. 141 (1994) L108.
[9] T. Osaka, T. Momma, T. Tajima, Y. Matsumoto, J. Electrochem. Soc. 142 (1995) 1057.
[10] J.O. Besenhard, G. Eichinger, J. Electroanal. Chem. 68 (1976) 1.
[11] S. Tobishima, J. Yamaki, A. Yamaji, T. Okada, J. Power Sources 13 (1984) 261.
[12] S. Tobishima, T. Okada, Electrochim. Acta. 30 (1985) 1715.
[13] S. Tobishima, T. Okada, J. Appl. Electrochem. 15 (1985) 317.
[14] S. Tobishima, J. Yamaki, T. Okada, Denki Kagaku 53 (1985) 173.
[15] C. Fringant, A. Tranchant, R. Messina, Electrochim. Acta 40 (1995) 513.
[16] H. Koshina, N. Eda, A. Morita, Extended Abstracts of 40th ISE Meeting, 19-02-14-G, Int. Soc. of Electrochem., Kyoto, Japan, September 17–22, 1989, p. 520.
[17] T. Matsui, K. Takeyama, Extended Abstracts of the 34th Battery Symposium in Japan, The Electrochem. Soc. in Japan, Hiroshima Japan, November 22–24, 1993, p. 29.
[18] T. Matsui, K. Takeyama, Extended Abstracts of the 35th Battery Symposium in Japan, The Electrochem. Soc. in Japan, Nagoya, Japan, November 14–16, 1994, p. 95.
[19] K. Morigaki, N. Kabuto, K. Yoshino, A. Ohta, Extended Abstracts of the 35th Battery Symposium in Japan, The Electrochem. Soc. in Japan, Nagoya, Japan, November 14–16, 1994, p. 83.
[20] M. Mori, Y. Shinagawa, T. Suzuki, K. Naoi, Extended Abstracts of the 36th Battery Symposium in Japan, The Electrochem. Soc. in Japan, Kyoto, Japan, September 12–14, 1995, p. 169.
[21] J.A.R. Stiles, K. Brandt, Canada Pat. 1190279 (1985).
[22] D.P. Wilkinson, H. Blom, K. Brandt, D. Wainwright, J. Power Sources 36 (1991) 517.
[23] F.R.N. Nabarro, P.J. Jackson, Growth and perfection of crystals, Proc. Int. Conf. on Crystal Growth, Cooperstown, NY, August 27–29, 1958, p. 13.
[24] W. Dittmar, K. Neumann, Growth and perfection of crystals, Proc. Int. Conf. on Crystal Growth, Cooperstown, NY, August 27–29, 1958, p. 121.
[25] R.H. Doremus, B.W. Roberts, D. Turnbull (Eds.), Growth and perfection of crystals, Proc. Int. Conf. on Crystal Growth, Cooperstown, NY, August 27–29, 1958.
[26] J. Franks, Acta Metallurgica 6 (1958) 103.
[27] K.N. Tu, Phys. Rev. B 49 (1994) 2030.
[28] D. Aurbach, A. Zaban, Y. Gofer, Y.E. Ely, I. Weissman, O. Chusid, O. Abramson, J. Power Sources 54 (1995) 76.
[29] J. Yamaki, K. Hayashi, K. Saito, T. Shodai, M. Arakawa, S. Tobishima, Extended abstracts, 188th Electrochem. Soc. Meeting, Abstract No. 84, Chicago, IL, USA, October (1995).
[30] E. Peled, J. Electrochem. Soc. 126 (1979) 2047.
[31] E. Ben-Jacob, R. Godbey, N.D. Goldenfeld, J. Koplik, H. Levine, T. Mueller, L.M. Sander, Phys. Rev. Lett. 55 (1985) 1315.
[32] J. Yamaki, Y. Katayama, J. Appl. Polym. Soc. 19 (1975) 2897.
[33] H. Margenau, G.M. Murphy, The Mathematics of Physics and Chemistry, D. Van Nostrand, Chap. 2.2.i (1943).
[34] D.P. Wilkinson, H. Blom, K. Brandt, Proc. 5th Int. Meeting on Lithium Batteries, Beijing, China, May 27–June 1, 1990, p. 145.
[35] Chem. Soc. Japan (Ed.), Kaitei 3 Pann, Kagaku Binnrann, Kisohenn II (in Japanese), Maruzen, Chap. 7, p. II–81 (1984).